

Article

# Effect of MgO and K<sub>2</sub>O on High-Al Silicon–Manganese Alloy Slag Viscosity and Structure

Xiangdong Xing<sup>1,2</sup>, Zhuogang Pang<sup>1,2</sup>, Jianlu Zheng<sup>1</sup>, Yueli Du<sup>1</sup>, Shan Ren<sup>3,\*</sup> and Jiantao Ju<sup>1,2,\*</sup>

<sup>1</sup> School of Metallurgical Engineering, Xi'an University of Architecture and Technology, Xi'an 710055, China; xaxxd@xauat.edu.cn (X.X.); hjpangzhuogang@163.com (Z.P.); zhengjianlud@163.com (J.Z.); 18821795206@163.com (Y.D.)

<sup>2</sup> Metallurgical Engineering Technology Research Center of Shaanxi Province, Xi'an 710055, China

<sup>3</sup> College of Materials Science and Engineering, Chongqing University, Chongqing 400044, China

\* Correspondence: shan.ren@cqu.edu.cn (S.R.); jiguangheng@xauat.edu.cn (J.J.)

Received: 28 July 2020; Accepted: 8 September 2020; Published: 14 September 2020



**Abstract:** The viscosity, melting properties, and molten structure of the high-Al silicon–manganese slag of SiO<sub>2</sub>–CaO–25 mass% Al<sub>2</sub>O<sub>3</sub>–MgO–MnO–K<sub>2</sub>O system with a varying MgO and K<sub>2</sub>O content were studied. The results show that with the increase in MgO content from 4 to 10 mass%, the measured viscosity and flow activation energy decreases, but K<sub>2</sub>O has an effect on increasing those of slags. However, the melting temperature increases due to the formation of high-melting-point phase spinel. Meanwhile, Fourier transform infrared (FTIR) and X-ray photoelectron spectra (XPS) were conducted to understand the variation of slag structure. The O<sup>2-</sup> dissociates from MgO can interact with the O<sup>0</sup> within Si–O or Al–O network structures, corresponding to the decrease in the trough depth of [SiO<sub>4</sub>] tetrahedral and [AlO<sub>4</sub>] tetrahedral. However, when K<sub>2</sub>O is added into the molten slag, the K<sup>+</sup> can accelerate the formation of [AlO<sub>4</sub>] tetrahedra, resulting in the increase in O<sup>0</sup> and O<sup>-</sup> and the polymerization of the structure.

**Keywords:** viscosity; structure; silicon–manganese slag; melting properties

## 1. Introduction

Nowadays, the silicomanganese (SiMn) alloy, a common deoxidant and desulfurizer, has been widely used in most steels containing silicon and manganese [1]. Calcium-based silicomanganese slag is primarily adopted in the production of SiMn because it easily controls the furnace conditions and alloy composition, but a large amount of slag will be generated and reduce the recovery of Si and Mn. In this case, many plants have begun to produce silicomanganese alloys using high-alumina slag ( $\geq 15$  mass% Al<sub>2</sub>O<sub>3</sub>) to improve the recovery rate of Si and Mn elements and reduce the slag production as well as energy consumption. Meanwhile, as the consumption of high-quality manganese ores, the cost of raw materials for manganese ferroalloys producers gradually rises, which increases the utilization of low-grade, low-cost materials, but it also leads to the increase in the content of Al<sub>2</sub>O<sub>3</sub> and alkaline oxides such as K<sub>2</sub>O in silicomanganese alloys slags.

In the production of SiMn, the viscous behavior of molten slag is one of the most crucial factors that affects not only the smelting process, but also the reaction kinetics and the mass/heat transfer [2]. For instance, when viscosity increases significantly, it will delay the transfer of silicon and manganese between slag and metal, as well as the final slag removal. Controlling the viscosity of the slag within an appropriate range can ensure that slags have good fluidity and increase the amount of MnO and SiO<sub>2</sub> reduced from the slag to the alloy. However, the increment of Al<sub>2</sub>O<sub>3</sub> and K<sub>2</sub>O content in the slag

will significantly increase viscosity, resulting in many operating and product quality problems. MgO is the main compound in slag, and an appropriate increase in its content can improve the fluidity of the slag. Thus, in the present study, we aimed to adjust the MgO content of slag to alleviate the increment in the viscosity of slag with high aluminum and potassium.

Previous works by the present authors [3] found that MgO decreased the viscosity and break temperature of BaO-bearing blast furnace (BF) slag. The results of Sun et al. [4] indicated that MgO provided oxygen ions to the molten slag which caused the depolymerization of the complex structure into simple units, resulting in decreasing the viscosity of SiO<sub>2</sub>–CaO–17 mass% Al<sub>2</sub>O<sub>3</sub>–MgO slag, while the viscosity increased when MgO content exceeded 10 mass%. Yao et al. [5] investigated the structure of high alumina blast furnace slag, and found that Si–O tetrahedral linked together to form the network structure, and basic oxides (MgO) could destroy the complex polymerization. Otherwise, Liu et al. [6] studied the effect of K<sub>2</sub>O on the viscosity and structure of CaO–SiO<sub>2</sub>–8 mass% MgO–17 mass% Al<sub>2</sub>O<sub>3</sub>–2.5 mass% BaO–K<sub>2</sub>O slag and revealed that K<sub>2</sub>O increased the polymerization degree of aluminosilicate anions, which increased slag viscosity. Zhang et al. [7] suggested that the K<sup>+</sup> compensated Al<sup>3+</sup> to form a bridging oxygen bond O<sub>Al,K</sub>, which is stronger than O<sub>Al,Ca</sub>, increasing the slag viscosity, and reached a maximum at K<sub>2</sub>O/Al<sub>2</sub>O<sub>3</sub> > 1. Although research works related to the influence of MgO and K<sub>2</sub>O on the viscosity and structure of blast furnace slag have been implemented, the data of that on the unique SiO<sub>2</sub>–CaO–Al<sub>2</sub>O<sub>3</sub>–MgO–MnO–K<sub>2</sub>O silicomanganese alloys slag with a content of 25 mass% Al<sub>2</sub>O<sub>3</sub> is still lacking.

In this study, the effect of MgO and K<sub>2</sub>O content on the viscosity of silicomanganese alloy slag with 25 mass% Al<sub>2</sub>O<sub>3</sub> at a fixed CaO/SiO<sub>2</sub> mass ratio of 0.65 was investigated using the rotating spindle method. In addition, the melting properties of the slag were also analyzed. To correlate the effect of MgO and K<sub>2</sub>O on the viscosity and structure, Fourier transform infrared (FTIR) spectroscopy and X-ray photoelectron spectroscopy (XPS) of the slag were performed to understand the structural rule of the slags.

## 2. Experimental

### 2.1. Materials Preparation

In this study, the chemical composition of Al<sub>2</sub>O<sub>3</sub>-based SiMn alloy slag was first analyzed by X-ray fluorescence (XRF, S4 Explorer; Bruker AXS, Karlsruhe, Germany), and the result was shown in Table 1. Based on the information of Table 1, the experimental slag samples were synthesized using reagent grade chemicals of SiO<sub>2</sub>, CaO, Al<sub>2</sub>O<sub>3</sub>, MgO, MnO, and K<sub>2</sub>CO<sub>3</sub>. The target compositions of the experimental samples are listed in Table 2, and the basicity of all synthesized samples was fixed at 0.65. The raw materials precisely weighed 180 g to form the given compositions and were then mixed thoroughly in a mortar. Thereafter, the mixture was placed into a Mo crucible and pre-melted at 1600 °C under Ar (99.99%, 0.25 L/min) atmosphere. After keeping 1600 °C for 180 min, to obtain uniform melt, it was poured into water. Then, the quenched sample was collected and dried.

### 2.2. Measurement of Viscosity

The slag viscosity measurements were conducted using the rotating cylinder method. The schematic figure of the viscosity measurement equipment can be seen in the previous work [3]. The apparatus mainly consists of five U-shaped MoSi<sub>2</sub> heating components, a Pt–6% Rh and Pt–30% Rh thermocouple (the error < ±2 °C), a Mo rotor, and a differential transformer. The quenched samples were melted at 1600 °C and kept for 30 min to obtain a homogeneous liquid phase. The spindle was then immersed into the liquid slag. Thereafter, the furnace was cooled down slowly from 1600 °C at the rate of 5 °C/min. The viscosity measurements were performed at intervals of 20 °C during the cooling cycle. The measurements were conducted until the viscosity value of melt > 5 Pa·s. The viscosity–time curve was recorded by the software. There was very little Mo (<0.05 mass%) infiltrated into the slag, which

has an ignorable effect on the viscosity of molten slags. The viscosity measurement equipment was calibrated by castor oil before each experiment.

**Table 1.** Chemical composition of high-Al silicon–manganese alloy slag.

Composition	SiO <sub>2</sub>	CaO	Al <sub>2</sub> O <sub>3</sub>	MnO	MgO	K <sub>2</sub> O	Other
Mass%	38.54	26.21	22.87	4.24	3.97	0.32	3.85

**Table 2.** The intended composition of the synthesized sample.

Sample	SiO <sub>2</sub>	CaO	Al <sub>2</sub> O <sub>3</sub>	MnO	MgO	K <sub>2</sub> O	Basicity
	(mass%)	(mass%)	(mass%)	(mass%)	(mass%)	(mass%)	(CaO/SiO <sub>2</sub> )
1	38.79	25.21	25	5	4	2	0.65
2	37.58	24.42	25	5	6	2	0.65
3	36.36	23.64	25	5	8	2	0.65
4	35.15	22.85	25	5	10	2	0.65
5	36.97	24.03	25	5	8	1	0.65
6	35.76	23.24	25	5	8	3	0.65
7	35.15	22.85	25	5	8	4	0.65

### 2.3. Measurement of Melting Properties

The melting properties of slags were determined by a melting-point and melting-rate comprehensive measurement system. (MTLQ-RD-1600, Chongqing University of Science and Technology, Chongqing, China), as illustrated in Figure 1. The system mainly included a high-temperature furnace, a charge coupled device (CCD) camera, a cooling water tank, and an analysis computer. The height of the cylindrical slag sample ( $\Phi 3 \times 3 \text{ mm}^2$ ) was reduced during the heating process (the heating rate was  $15 \text{ }^\circ\text{C}/\text{min}$ ). The analysis computer recorded the temperature at which the height of the sample reduced to 75%, 50%, and 25% of the initial height as the softening, hemispherical, and flow temperature, respectively. Each sample was tested three times and we calculated the average values of the experiment.

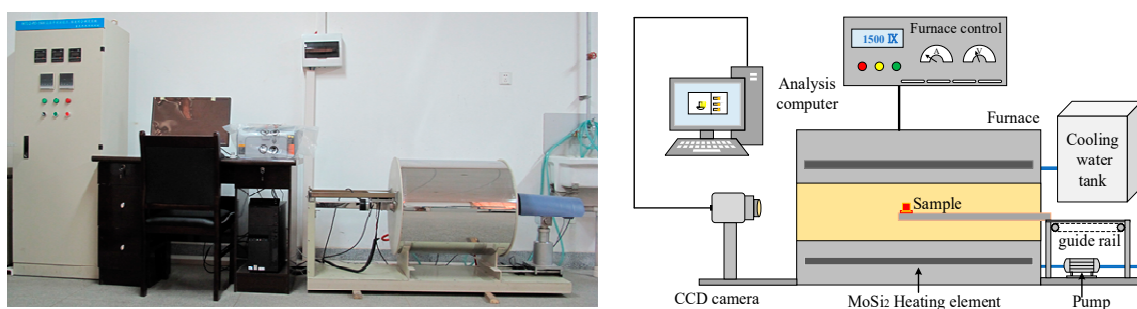


**Figure 1.** The schematic figure of melting-point and melting-rate comprehensive measurement system.

### 2.4. Measurement of Structure

All the samples were pre-melted at  $1600 \text{ }^\circ\text{C}$  and quenched in water to maintain the slag's molten structural state. The quenched powders ( $\sim 200$  mesh) were conducted by X-ray diffraction (XRD, D8 Advance A25; Bruker AXS, Karlsruhe, Germany) for ensuring the state of the slag. The XRD used a Cu K $\alpha$  radiation at a scan rate of  $3^\circ/\text{min}$  over the degree of  $20\text{--}90^\circ$ , and the XRD patterns are presented in Figure 2. There are no characteristic peaks that can be detected in Figure 2, suggesting that the samples were amorphous. The quenched samples were used to analyze the slag structure through FTIR (Nicolet iS5; Thermo Fisher Scientific, Waltham, MA, USA) and XPS (EscaLab Xi+, Thermo Fisher Scientific,

Waltham, MA, USA) spectroscopy. During the FTIR measurement, 2.0 mg sample (−300 mesh) and 300 mg KBr were mixed, and then the mixture was pressed into a film. The sample was recorded at a scope of 400–4000  $\text{cm}^{-1}$  with a resolution of 4  $\text{cm}^{-1}$ . Each sample was scanned for 32 s. In addition, XPS was carried out at a vacuum chamber with  $8 \times 10^{-10}$  Pa and used an Al K $\alpha$  monochromatic source (1486.6 eV). The O<sub>1s</sub> peak was deconvoluted and peak fitted using XPS Peak (Version 4.1) and Origin software (Version 2019). The peaks were appropriately calibrated by the C<sub>1s</sub> of externally doped carbon as the reference peak, and the binding energy of C<sub>1s</sub> is 284.80 eV.

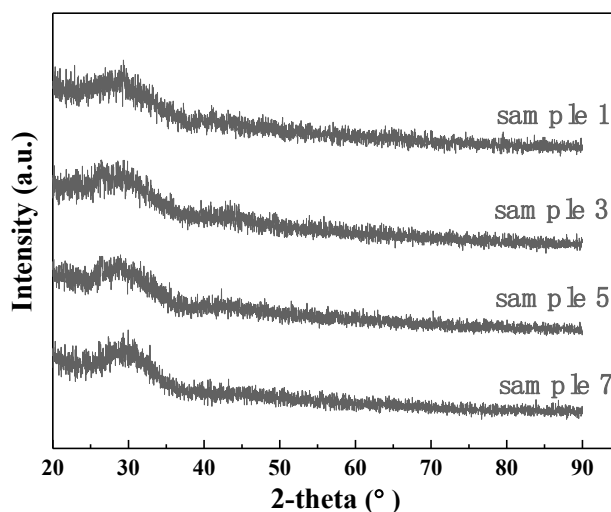


Figure 2. The XRD pattern of quenched slags.

### 3. Results and Discussion

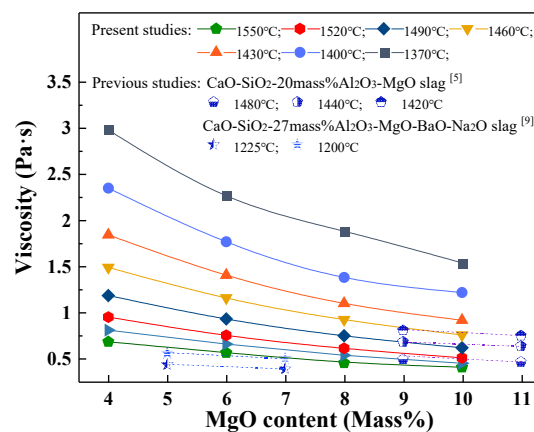
#### 3.1. Viscosity of Slag

Figure 3 graphically shows the viscosity of the SiO<sub>2</sub>–CaO–25 mass% Al<sub>2</sub>O<sub>3</sub>–MnO–MgO–K<sub>2</sub>O system with a varying MgO content at a fixed basicity of 0.65. It can be clearly observed that the slag viscosity decreases with the addition of MgO content in the temperature range from 1370 °C to 1550 °C, and the decreasing rate of viscosity slows down when the MgO content exceeds 8 mass%. For example, the average decrement of viscosity is 0.284 Pa·s with the increment of MgO from 4 to 8 mass% at 1460 °C, whereas the viscosity just decreases by 0.168 Pa·s as the MgO content increases from 8 to 10 mass%. The viscous values of previous studies related to high Al<sub>2</sub>O<sub>3</sub> containing slag are also included in Figure 3 [5,8,9]. Though the slag compositions are different, it exhibits a similar trend of slag viscosity to that of this study. However, it can be noted that the viscosity values of slag are lower than that of the present study, which is attributed to the high basicity (CaO/SiO<sub>2</sub> > 1.0). Work performed by Li et al. [10] suggested that MgO depolymerized the complex silicate and aluminate network structure, and then decreased viscosity. According to Kim et al. [11], MgO is classified as basic oxide and acted as a network modifier, and much of the network structure units were depolymerized into dimer or monomer units, as expressed by Equation (1):



The viscosity for samples 3, 5, 6, and 7 with varying K<sub>2</sub>O contents is shown in Figure 4. On the contrary of MgO, K<sub>2</sub>O tends to increase the viscosity of slag. The effect of K<sub>2</sub>O is relatively weak when the temperature is higher than 1520 °C, which is because the excess thermal energy had sufficiently modified the intricate network structure of the slag, and large amounts of simpler structural units exist in molten slag. The same variation trends of slag viscosity with the addition of K<sub>2</sub>O are found within the works of Liu et al. [6] and Chang et al. [12]. Generally, K<sub>2</sub>O is classified as basic oxide

which will introduce free oxygen ( $O^{2-}$ ) to destroy Si–O bonds within an intricate silicate network, leading to the increment of non-bridging oxygens and eventually lowering slag viscosity. However, the result is in contradiction with the trend of viscosity of present slag, indicating that some other effects of  $K_2O$  have more significant influence on slag viscosity. Based on the previous literature [7,12], it can be speculated that  $Al^{3+}$  prefers to form  $AlO_4^{5-}$  tetrahedrons and the process needs cations (such as  $K^+$  or  $Ca^{2+}$ ) to maintain electroneutrality, which is called charge compensation. However,  $K^+$  possesses higher priority than  $Ca^{2+}$  to compensate  $Al^{3+}$ , leading to  $K^+$  gradually substituting  $Ca^{2+}$  and transforming  $O_{Al,Ca}$  to  $O_{Al,K}$ . Since the length of chemical bonds between Al and Ca ( $\alpha_{Al,Ca} = 4.996$ ) are longer than those between Al and K ( $\alpha_{Al,K} = 4.156$ ), the chemical bonds around  $O_{Al,K}$  are stronger than those around  $O_{Al,Ca}$ . Thus, the charge compensation leads to an increase in the stability of slag structure and increases the slag viscosity. Considering the increment of viscosity under the condition of  $K_2O$ , the effect of  $K^+$  seems to be more dominating. From the results of slag viscosity with different MgO and  $K_2O$  content, the addition of MgO is limited to the range of 6–8 mass%, and  $K_2O$  content should be controlled below 1 mass%, for the production of SiMn alloys.



**Figure 3.** MgO content dependence on the viscosity of the slags at the temperature between 1370 °C and 1550 °C.

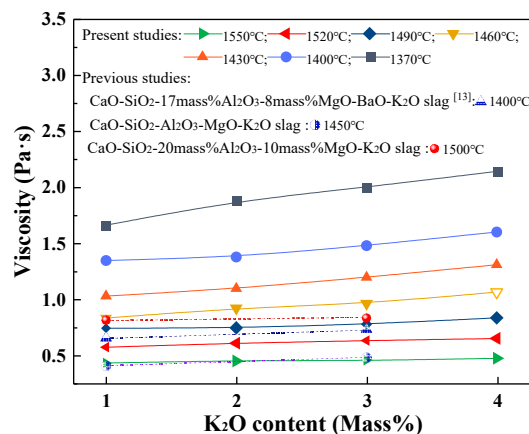


**Figure 4.**  $K_2O$  content dependence on the viscosity of the slags at the temperature between 1370 °C and 1550 °C.

In addition, the volume fractions of liquid and solid phases were calculated by Factsage thermodynamic software, and the results of calculation were presented in Tables S1–S7 and Figure S1 that were attached in the Supplementary Material. It should be mentioned that there are solid precipitates during the viscosity measurement, and the maximum amount of precipitation is 10%.

### 3.2. Flow Activation Energy

In general, the variation of viscosity is related to the flow activation energy that represents the energy barrier to overcome the shear stress for liquid melt movement [13]. The viscosity of slag is affected by the temperature, and the Weymann–Frenkel equation is usually adopted to describe the relationship between the two, as expressed as Equation (2) [14]. This can be taken logarithmically and written as Equation (3):

$$\eta = \eta_0 + \text{Exp}\left(\frac{E_f}{RT}\right) \quad (2)$$

$$\ln(\eta) = \ln(\eta_0) + \left(\frac{E_f}{RT}\right) \quad (3)$$

where  $\eta$ ,  $\eta_0$ ,  $E_f$ ,  $R$ , and  $T$  are the viscosity of the slag in Pa·s, the pre-exponential constant, the flow activation energy in J/mol, the ideal gas constant of  $8.314 \text{ J}\cdot(\text{mol}\cdot\text{K})^{-1}$ , and the absolute temperature in K, respectively. The values of  $E_f$  are calculated on the basis of the slope of the fitting line depicted in Figure 5. Table 3 lists the results of the calculation.

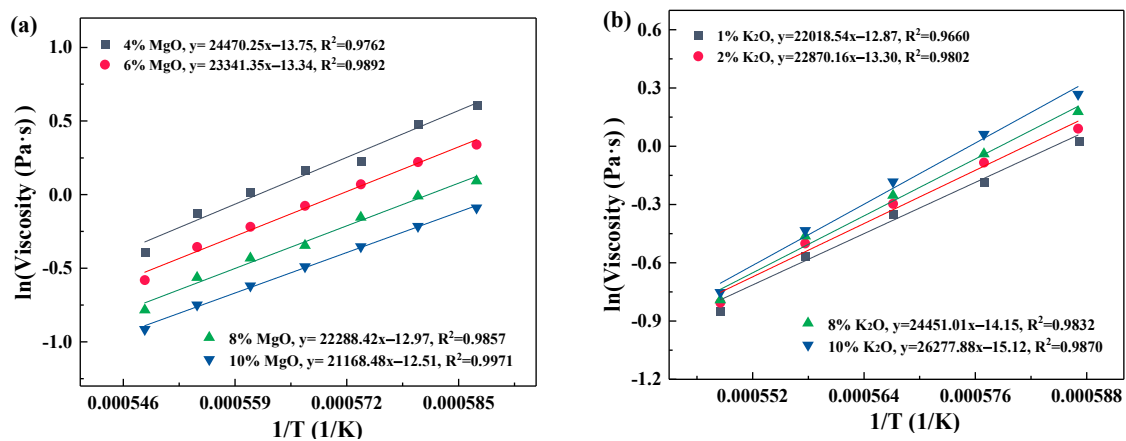


**Figure 5.** The reciprocal of temperature dependence on the viscosity of the slags (a) with a varying MgO content; and (b) with a varying K<sub>2</sub>O content.

**Table 3.** The calculated results of apparent activation energy.

MgO (mass%)	$E_f$ (kJ/mol)	K <sub>2</sub> O (mass%)	$E_f$ (kJ/mol)
4	$203.45 \pm 12.95$	1	$183.06 \pm 17.10$
6	$194.06 \pm 8.29$	2	$190.14 \pm 13.50$
8	$185.31 \pm 9.11$	3	$203.29 \pm 13.27$
10	$175.99 \pm 3.86$	4	$218.47 \pm 12.51$

As shown in Figure 5 and Table 3, the variation of  $E_f$  shows good agreement with that of viscosity. The flow activation energy increases with increasing K<sub>2</sub>O content, while MgO has an effect on diminishing the values of  $E_f$ . This indicates that with the increase in MgO content, the complex structure transforms into simpler units which leads to a decline in the energy barrier for viscous flow, whereas K<sub>2</sub>O increases the resistance of melt flows due to the polymerization of the structural units. The viscosity of silicate–aluminat melt is predominantly determined by its structure at high temperature, and many spectroscopic methods have been developed to identify the ionic structural units. Moreover, the FTIR spectroscopy and XPS were conducted in the present study.

### 3.3. Structure Analysis of the Slag Using FTIR Spectroscopy

The viscosity of slag is closely related to its structure. Generally, the viscosity increases when the complexity of the structure increases, but it decreases when the simple structural units are formed. Figure 6 presents the FTIR transmittance spectra of glassy samples with different MgO content. The symmetric stretching bands of  $[\text{SiO}_4]$  tetrahedra are detected between  $1200$  and  $750\text{ cm}^{-1}$ , and it is generally divided into four typical bands assign to  $Q^0$  ( $[\text{SiO}_4]^{4-}$ , monomer,  $880\text{--}850\text{ cm}^{-1}$ ),  $Q^1$  ( $[\text{SiO}_4]^{4-}$ , dimers,  $920\text{--}900\text{ cm}^{-1}$ ),  $Q^2$  ( $[\text{Si}_2\text{O}_7]^{6-}$ , chains,  $1000\text{--}950\text{ cm}^{-1}$ ), and  $Q^3$  ( $[\text{Si}_3\text{O}_{10}]^{8-}$ , sheets,  $1100\text{--}1050\text{ cm}^{-1}$ ), respectively [3,9,15,16]. It can be observed that as the MgO content is increased, the transmission trough between  $1200\text{--}750\text{ cm}^{-1}$  becomes regularly shallower. This suggests that the silicate structures are depolymerized under the action of MgO. In addition, the significant differences for both of the trough of  $[\text{AlO}_4]$  tetrahedra and Si–O–Al are also ascertained. The curves of the  $[\text{AlO}_4]$  tetrahedral band get smooth, indicating that MgO also plays a role of modifier on the aluminate network and decreases the relative fraction of the  $[\text{AlO}_4]$  tetrahedral units within the melt. According to the work of Qi et al., [15] the bridging oxygen in  $[\text{AlO}_4]$  tetrahedra can be transformed to non-bridging oxygen, which suggests the decrease in the degree of polymerization of slag, and the transformation is expressed by Equations (4) and (5). Meanwhile, the decline depth of the Si–O–Al trough further illustrates the number of complex structures formed by the combination of  $[\text{SiO}_4]$  tetrahedra and  $[\text{AlO}_4]$  tetrahedra is reduced, that is, the complex network structure is depolymerized.

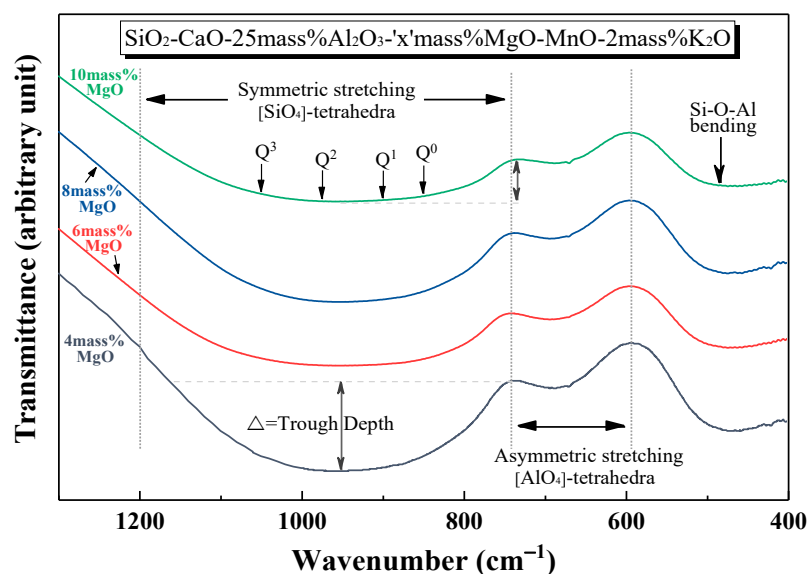


**Figure 6.** The effect of the MgO on the FTIR spectra of  $\text{SiO}_2\text{--CaO--}25\text{ mass\% Al}_2\text{O}_3\text{--MnO--MgO--}2\text{ mass\% K}_2\text{O}$  slag.

The FTIR spectra for glassy samples with varying  $\text{K}_2\text{O}$  content are shown in Figure 7. Though the band group of  $[\text{SiO}_4]$  tetrahedral stretching between  $1200$  and  $750\text{ cm}^{-1}$  deepens slightly with the addition of  $\text{K}_2\text{O}$ , the center of the trough declines from  $961$  to  $938\text{ cm}^{-1}$ , which is presumably due to the formation of simpler Si–O structures, but it will cause the slag viscosity to decrease. In fact, the experimental viscosity of the slag is contrary to the aforementioned speculation. It can be noted that as the  $\text{K}_2\text{O}$  content increases, the shoulder at nearly  $736\text{ cm}^{-1}$  gradually moves to higher wavenumbers, broadening the  $[\text{AlO}_4]$  tetrahedral trough, and the depth increases from  $h_1$  (0.95) to  $h_2$  (2.8). In addition, the Si–O–Al bending troughs identified by the trough at nearly  $480\text{ cm}^{-1}$  also

shifts to a higher wavenumber. The results indicate that  $K_2O$  has a different effect on  $[SiO_4]$  tetrahedral and  $[AlO_4]$  tetrahedral structures. According to Sohn et al. [17],  $K_2O$  can accelerate the formation of  $[AlO_4]$  tetrahedra that acts as a network former, which can be expressed by Equation (6). Combining the results of the viscosity experiment and the analysis of the FTIR spectra, it can be inferred that  $K_2O$  has more effect on aluminate structures to form network structure:

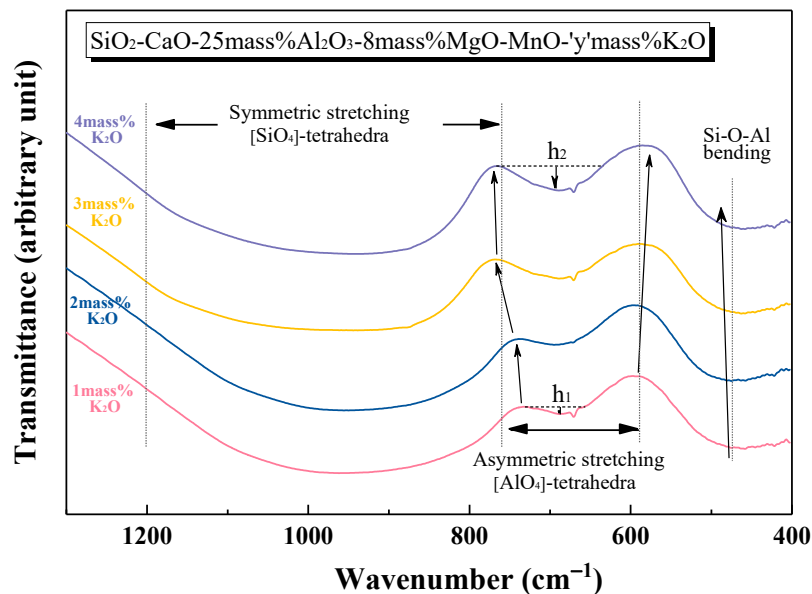
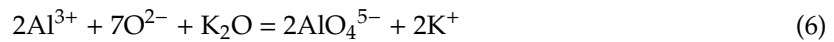


**Figure 7.** The effect of  $K_2O$  on the FTIR spectra of  $SiO_2$ - $CaO$ -25 mass%  $Al_2O_3$ -8 mass%  $MgO$ - $MnO$ - $K_2O$  slag.

### 3.4. Structure Analysis of the Slag Using XPS

To elucidate the influence of  $K_2O$  and  $MgO$  on the structure of the  $SiO_2$ - $CaO$ - $Al_2O_3$ - $MnO$ - $MgO$ - $K_2O$  system, the amorphous quenched samples were analyzed, as was the main  $O_{1s}$  peak, using XPS. According to the studies of Kim et al. [18] and Wu et al. [19], three different types of oxygens exist in silicate melts, which are bridging oxygen (BO,  $O^0$ , connected to two  $Si^{4+}$ ), non-bridging oxygen (NBO,  $O^-$ , connected to a  $Si^{4+}$ ), and free oxygen (FO,  $O^{2-}$ , not connected with silicon cations), respectively. The fraction variation of different types of oxygen ions can provide a detailed bonding complexity of the melt. For instance, the higher the amount of bridging oxygen, the more the structural units (Si-O or Al-O) are connected, and the greater the degree of polymerization (DOP) of slag.

Figure 8 shows the deconvoluted result of the  $O_{1s}$  binding energy from the XPS, and the background is removed using Shirley's method. The binding energy, of nearly 530.3 eV, 531.3 eV, and 532.2 eV, assigned to FO, NBO, and BO, respectively, which is close to that observed by Wang et al. [20] and Kim and Shon. [18] From Figure 8a, the intensity peaks corresponding to different oxygen ion species change significantly with  $MgO$  additions. In particular, the  $O^{2-}$  always takes up a relatively large portion, and the fraction of  $O^0$  gradually decreases with the addition of  $MgO$ . Additionally, it can be seen that the portion of  $O^-$  firstly enlarges with the content of  $MgO$  increasing from 4 to 6 mass%, and then decreases by further adding  $MgO$ . On the contrary,  $K_2O$  plays a role in increasing the amount of  $O^0$  and  $O^-$ , leading to the higher DOP of slag. By calculating the integrated areas of the deconvoluted peaks, the relative fractions of  $O^0$ ,  $O^-$ , and  $O^{2-}$  can be observed visually, and the results of the calculation are depicted in Figure 9. According to Figure 9a, the fraction of  $O^{2-}$  increases from 41.25% to 49.35% with the  $MgO$  content up of to 10 mass%, while the average decrement of the fraction of  $O^0$ , and  $O^-$  are

2.29% and 0.41%. It further suggests that MgO can dissociate free oxygen ( $O^{2-}$ ) and it interacts with the bridging oxygen ( $O^0$ ) to create the simpler non-bridging oxygen ( $O^-$ ), as expressed by Equation (7), which weakens the complexity of slag structure. It can note that by increasing the content of MgO from 8 to 10 mass%, the relative fraction of  $O^0$  did not obviously reduce, which leads us to speculate that the bridging oxygen has already been depolymerized by  $O^{2-}$ , hence the reduction becomes less noticeable. Besides, the effect of  $K_2O$  on the fractions of oxygen species is presented in Figure 9b. The fraction of BO and NBO increases from 21.17% to 26.11% and from 33.42% to 34.29%, respectively. Based on the aforementioned analysis of FTIR spectra, the increment of BO and NBO is attributed to  $K_2O$  improving the formation of the  $[AlO_4]$  tetrahedral that acts as a network former. Thus, the slag structure becomes intricate, and the viscosity is higher, which is consistent with the results of the viscous measurement:

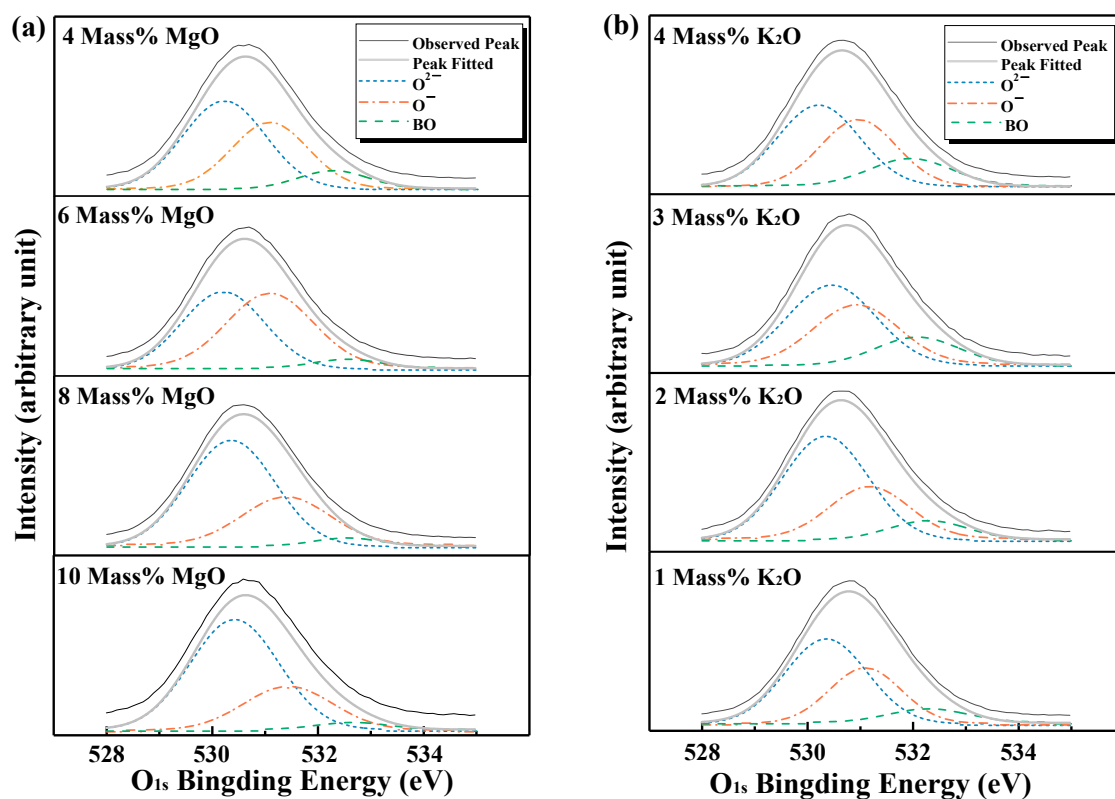


**Figure 8.** The  $O_{1s}$  XPS spectra for  $SiO_2$ - $CaO$ -25 mass%  $Al_2O_3$ -8 mass%  $MgO$ - $MnO$ - $K_2O$  slag as function of binding energy (a) with varying  $MgO$  content; (b) with varying  $K_2O$  content; BO is Bridging oxygen.

### 3.5. Melting Properties of Slags

The composition of slag affects the melting properties of slags that are very important considerations in the SiMn production process. The influence of  $K_2O$  and  $MgO$  on the melting properties of  $SiO_2$ - $CaO$ - $Al_2O_3$ - $MnO$ - $MgO$ - $K_2O$  slag are shown in Figure 10. It is clear that the softening, hemispherical, and flowing temperatures of all slags rises with the increment of  $MgO$  and  $K_2O$  content. The flowing temperature ( $T_f$ ) can be considered as the liquid temperature (totally melted), and it increases from 1372 °C to 1428 °C with the addition of  $MgO$  at 2 mass%  $K_2O$ .  $MgO$  has an effect on decreasing slag viscosity, but has an opposite effect on the liquid temperature. Besides, with the increase in  $K_2O$  content, the  $T_h$  rises from 1389 °C to 1425 °C.

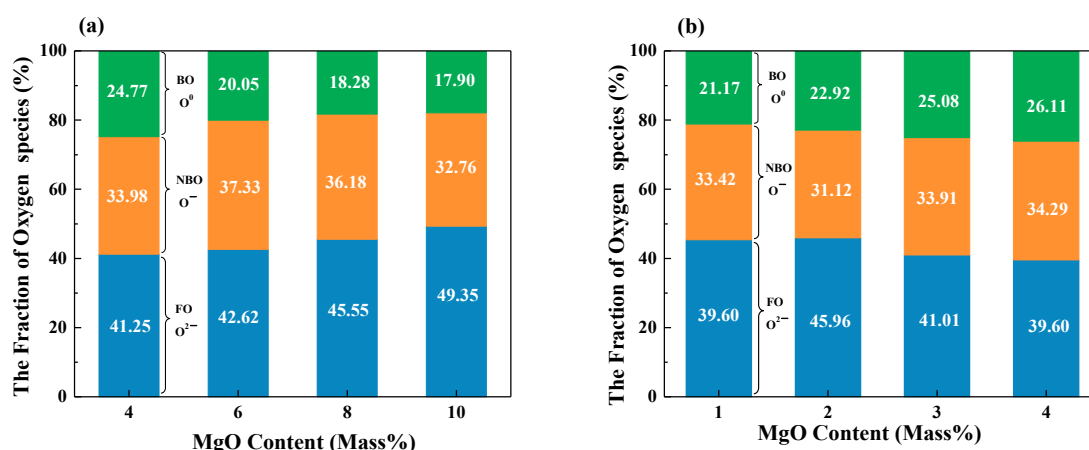


Figure 9. The fractions of the different types of oxygens (a) with a varying MgO content; and (b) with a varying K<sub>2</sub>O content.

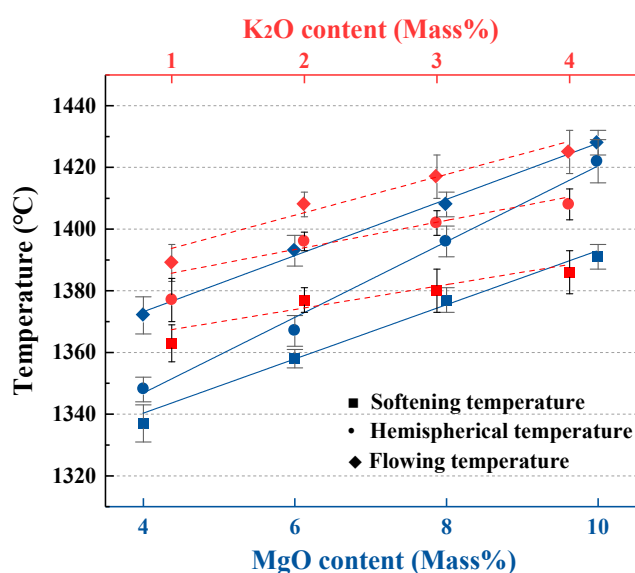
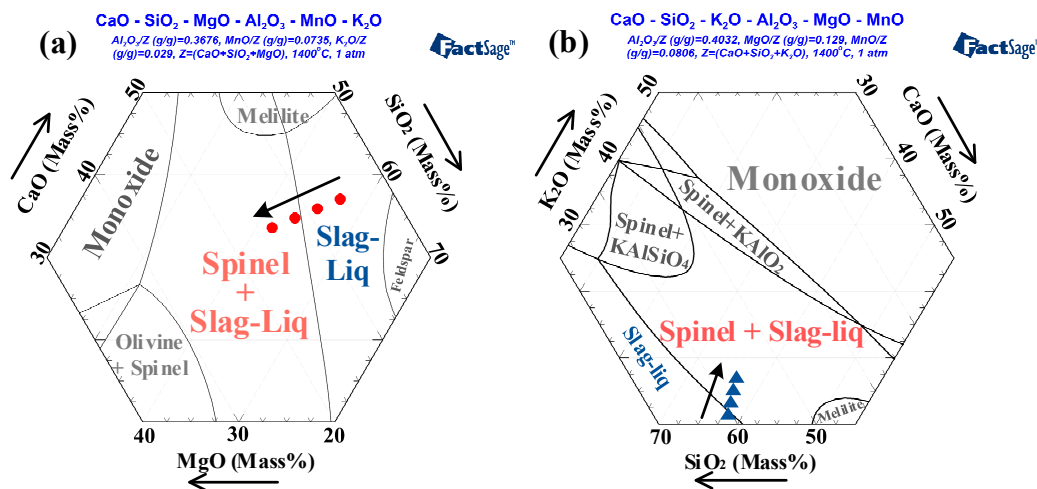


Figure 10. The effect of MgO and K<sub>2</sub>O on the melting properties of slags.

These phenomena can be explained from the phase diagram of the SiO<sub>2</sub>–CaO–Al<sub>2</sub>O<sub>3</sub>–MnO–MgO–K<sub>2</sub>O slag calculated by Factsage7.1 software, as shown in Figure 11. It was found from Figure 9a that the increase in MgO content leads to the transition from the liquid phase area to the spinel corresponding to the high melting point area, resulting in the increment of liquid temperature. The phase diagram in the condition of 8 mass% MgO varying with K<sub>2</sub>O is shown in Figure 9b, from which the phase moves from the liquid phase to the spinel phase with increasing K<sub>2</sub>O. Considering K<sub>2</sub>O not only increases the liquid temperature but also increases the slag viscosity, thus, the decreasing K<sub>2</sub>O content in the slag is beneficial to improve the melting speed and fluidity of the slag. Moreover, from the phase diagram, it is conducive to limit the content of MgO and K<sub>2</sub>O to less than 8 mass% and 1 mass%, respectively, for the slag with a low liquid temperature.



**Figure 11.** Phase diagram of SiO<sub>2</sub>–CaO–Al<sub>2</sub>O<sub>3</sub>–MnO–MgO–K<sub>2</sub>O slag system at 1400 °C: (a) with a varying MgO content; (b) with a varying K<sub>2</sub>O content.

#### 4. Conclusions

The viscosity, structure, and melting properties of high-Al silicon–manganese alloy slag with a varying K<sub>2</sub>O and MgO content were investigated in this study, and the main conclusions can be summarized as follows:

- (1) The viscosity of SiO<sub>2</sub>–CaO–25 mass% Al<sub>2</sub>O<sub>3</sub>–MgO–MnO–K<sub>2</sub>O slag decreases with the increment of MgO content, and the decreasing rate of viscosity slows down by further increasing the content of MgO from 8 to 10 mass%. However, the viscosity of slag increases with the increase in K<sub>2</sub>O.
- (2) MgO acts as a network modifier that can dissociate O<sup>2-</sup> and interact with the O<sup>0</sup> within Si–O or Al–O network structures, leading to an increase in the simpler O<sup>-</sup>, and then depolymerizes the complex network structure. On the contrary, when K<sub>2</sub>O is added into the molten slag, the K<sup>+</sup> can accelerate the formation of [AlO<sub>4</sub>] tetrahedra and connects aluminat–silicate structural units, which results in the increase in O<sup>0</sup> and O<sup>-</sup> and the polymerization of structure.
- (3) An increase in the MgO and K<sub>2</sub>O content leads to the transformation from the feldspar and liquid phase to spinel, which increases the melting temperature. By combining with the results of the viscosity and melting properties experiment, it is suitable to limit the content of MgO and K<sub>2</sub>O to less than 8 mass% and 1 mass%, respectively, for the production of silicon–manganese alloy.

**Supplementary Materials:** The following are available online at <http://www.mdpi.com/2075-163X/10/9/810/s1>, Figure S1: Relationship between the volume fraction of phases and calculated viscosity at different temperatures, Table S1: Calculation results of the liquid and solid phase fractions of sample 1#, Table S2: Calculation results of the liquid and solid phase fractions of sample 2#, Table S3: Calculation results of the liquid and solid phase fractions of sample 3#, Table S4: Calculation results of the liquid and solid phase fractions of sample 4#, Table S5: Calculation results of the liquid and solid phase fractions of sample 5#, Table S6: Calculation results of the liquid and solid phase fractions of sample 6#, Table S7: Calculation results of the liquid and solid phase fractions of sample 7#.

**Author Contributions:** Conceptualization, X.X. and Z.P.; methodology, X.X. and Z.P.; software, Z.P., S.R. and J.Z.; validation, Z.P., J.Z. and Y.D.; formal analysis, X.X. and Z.P.; investigation, X.X.; resources, X.X., Z.P. and J.J.; data curation, X.X. and Z.P.; writing—original draft preparation, X.X. and Z.P.; writing—review and editing, X.X.; supervision, X.X. and Z.P.; project administration, X.X.; funding acquisition, X.X. All authors have read and agreed to the published version of the manuscript.

**Funding:** The present work was financially supported by the National Natural Science Foundation of China (Grant No.51604209) and Natural Science Basic Research Program of Shaanxi (Program No. 2019JLP-05).

**Conflicts of Interest:** The authors declare no conflict of interest.

## References

1. Ahmed, A.; Ghali, S.; El-Fawakhry, M.K.; El-Faramawy, H.; Eissa, M. Silicomanganese Production Utilizing Local Manganese Ores and Manganese Rich Slag. *Ironmak. Steelmak.* **2013**, *41*, 310–320. [[CrossRef](#)]
2. Liu, Y.Y.; Lv, X.; Li, B.; Bai, C. Relationship between Structure and Viscosity of CaO–SiO<sub>2</sub>–MgO–30.00wt%–Al<sub>2</sub>O<sub>3</sub> Slag by Molecular Dynamics Simulation with FT–IR and Raman Spectroscopy. *Ironmak. Steelmak.* **2017**, *45*, 492–501. [[CrossRef](#)]
3. Xing, X.; Pang, Z.; Mo, C.; Wang, S.; Ju, J. Effect of MgO and BaO on Viscosity and Structure of Blast Furnace Slag. *J. Non-Cryst. Solids* **2020**, *530*, 119801. [[CrossRef](#)]
4. Sun, C.; Liu, X.; Li, J.; Yin, X.; Song, S.; Wang, Q. Influence of Al<sub>2</sub>O<sub>3</sub> and MgO on the Viscosity and Stability of CaO–MgO–SiO<sub>2</sub>–Al<sub>2</sub>O<sub>3</sub> Slags with CaO/SiO<sub>2</sub>=1.0. *ISIJ Int.* **2017**, *57*, 978–982. [[CrossRef](#)]
5. Yao, L.; Ren, S.; Wang, X.; Liu, Q.; Dong, L.; Yang, J.; Liu, J. Effect of Al<sub>2</sub>O<sub>3</sub>, MgO, and CaO/SiO<sub>2</sub> on Viscosity of High Alumina Blast Furnace Slag. *Steel Res. Int.* **2016**, *87*, 241–249. [[CrossRef](#)]
6. Liu, W.; Xing, X.; Zuo, H. The Viscous Behavior and Potassium Removal Capacity of CaO–SiO<sub>2</sub>–8wt%MgO–17wt%Al<sub>2</sub>O<sub>3</sub>–2.5wt%BaO–K<sub>2</sub>O Slag. *Metall. Res. Technol.* **2020**, *117*, 7.
7. Zhang, G.; Chou, K. Measuring and Modeling Viscosity of CaO–Al<sub>2</sub>O<sub>3</sub>–SiO<sub>2</sub>(–K<sub>2</sub>O) Melt. *Metall. Mater. Trans. B* **2012**, *43*, 841–848. [[CrossRef](#)]
8. Zhang, X.; Jiang, T.; Xue, X.; Hu, B. Influence of MgO/Al<sub>2</sub>O<sub>3</sub> Ratio on Viscosity of Blast Furnace Slag with High Al<sub>2</sub>O<sub>3</sub> Content. *Steel Res. Int.* **2016**, *87*, 87–94. [[CrossRef](#)]
9. Gao, E.; Wang, W.; Zhang, L. Effect of Alkaline Earth Metal Oxides on the Viscosity and Structure of the CaO–Al<sub>2</sub>O<sub>3</sub> Based Mold Flux for Casting High–Al Steels. *J. Non-Cryst. Solids* **2016**, *473*, 79–86. [[CrossRef](#)]
10. Li, P.; Ning, X. Effects of MgO/Al<sub>2</sub>O<sub>3</sub> Ratio and Basicity on the Viscosities of CaO–MgO–SiO<sub>2</sub>–Al<sub>2</sub>O<sub>3</sub> Slags: Experiments and Modeling. *Metall. Mater. Trans. B* **2016**, *47*, 446–457.
11. Kim, W.H.; Sohn, I.; Min, D.J. A Study on the Viscous Behaviour with K<sub>2</sub>O Additions in the CaO–SiO<sub>2</sub>–Al<sub>2</sub>O<sub>3</sub>–MgO–K<sub>2</sub>O Quinary Slag System. *Steel Res. Int.* **2010**, *81*, 735–741. [[CrossRef](#)]
12. Chang, Z.; Jiao, K.; Ning, X.; Zhang, J. Novel Approach to Studying Influences of Na<sub>2</sub>O and K<sub>2</sub>O Additions on Viscosity and Thermodynamic Properties of BF Slags. *Metall. Mater. Trans. B* **2019**, *50*, 1399–1406. [[CrossRef](#)]
13. Sun, Y.; Zhang, Z.; Liu, L.; Wang, X. FT–IR, Raman and NMR Investigation of CaO–SiO<sub>2</sub>–P<sub>2</sub>O<sub>5</sub> and CaO–SiO<sub>2</sub>–TiO<sub>2</sub>–P<sub>2</sub>O<sub>5</sub> Glasses. *J. Non-Cryst. Solids* **2015**, *420*, 26–33. [[CrossRef](#)]
14. Zhang, L.; Wang, W.; Xie, S.; Zhang, K.; Sohn, I. Effect of Basicity and B<sub>2</sub>O<sub>3</sub> on the Viscosity and Structure of Fluorine–Free Mold Flux. *J. Non-Cryst. Solids* **2017**, *460*, 113–118. [[CrossRef](#)]
15. Qi, J.; Liu, C.; Jiang, M. Role of Li<sub>2</sub>O on the structure and viscosity in CaO–Al<sub>2</sub>O<sub>3</sub>–Li<sub>2</sub>O–Ce<sub>2</sub>O<sub>3</sub> melts. *J. Non-Cryst. Solids* **2017**, *475*, 101–107. [[CrossRef](#)]
16. Zheng, K.; Zhang, Z.; Liu, L.; Wang, X. Investigation of the Viscosity and Structural Properties of CaO–SiO<sub>2</sub>–TiO<sub>2</sub> Slags. *Metall. Mater. Trans. B* **2014**, *45*, 1389–1397. [[CrossRef](#)]
17. Sohn, I.; Min, D.J. A Review of the Relationship between Viscosity and the Structure of Calcium–Silicate–Based Slags in Ironmaking. *Steel Res. Int.* **2012**, *83*, 611–637. [[CrossRef](#)]
18. Kim, H.; Sohn, I. Effect of CaF<sub>2</sub> and Li<sub>2</sub>O Additives on the Viscosity of CaO–SiO<sub>2</sub>–Na<sub>2</sub>O Slags. *ISIJ Int.* **2011**, *51*, 1–8. [[CrossRef](#)]
19. Wu, T.; Zhang, Y.; Yuan, F.; An, Z. Effects of the Cr<sub>2</sub>O<sub>3</sub> Content on the Viscosity of CaO–SiO<sub>2</sub>–10 Pct Al<sub>2</sub>O<sub>3</sub>–Cr<sub>2</sub>O<sub>3</sub> Quaternary Slag. *Metall. Mater. Trans. B* **2018**, *49*, 1719–1731. [[CrossRef](#)]
20. Wang, Z.; Sohn, I. Effect of substituting CaO with BaO on the viscosity and structure of CaO–BaO–SiO<sub>2</sub>–MgO–Al<sub>2</sub>O<sub>3</sub> slags. *J. Am. Ceram. Soc.* **2018**, *101*, 4285–4296. [[CrossRef](#)]

